Investigation of Oscillation Modes in a High-Speed Flow with Heat Supply. I. Experiment

N. N. Fedorova[a,*], **M. A. Goldfeld**[a], and **V. V. Pickalov**[a]

UDC 536.46

Abstract: Results of experimental investigations of the flow in a channel with sudden expansion without and with heat supply into a supersonic air flow are presented. Based on processing experimental data on the time evolution of static pressure on the channel walls, the spectral power of oscillations are determined. The analysis reveals an increase in the power spectral density of pressure oscillations in the frequency range of 250–400 Hz. The greatest increase in the spectral density is observed in the initial period of the process during ignition and at the end of flame stabilization. In the period corresponding to developed combustion, the peak value of the power spectrum of oscillations decreases, while the range of frequencies is extended to 400–600 Hz.

Keywords: supersonic flow, experiment, unsteady ignition, combustion, pressure oscillations, Fourier analysis.

INTRODUCTION

The analysis of flow oscillations and combustion instability in flows with heat supply is one of the general and urgent topics faced in the development of heaters and engines designed for various purposes [1, 2]. Combustion implementation often involves serious problems associated with instability of this process accompanied by intensification of pressure oscillations and certain resonance regimes. These problems are substantially aggravated as the combustion intensity increases.

With increasing flow velocity at the combustor channel entrance, the time of mixture residence in the combustor decreases, which requires additional efforts to ensure effective mixing and high combustion efficiency. This problem becomes more severe in the case of combustion at supersonic velocities of the flow in the channel [3]. In this case, various schemes of fuel injection are used, both intrusive and embedded, in various modifications [4], which are expected to improve mixing and assist in flame stabilization due to generation of recirculation zones and large-scale vortex structures. These devices serve as sources of powerful pressure oscillations generated under conditions of flow separation [5]. It is known that instability occurs owing to interaction of unsteady heat release during combustion and acoustic oscillations of pressure. As a result, there may occur unpredictable failure of the flame, mechanical and thermal damage of the combustor walls, and intense mechanical vibrations. To understand and prevent these phenomena, it is necessary to study the corresponding characteristics of the combustor as a dynamic system.

Spontaneous emergence of high-amplitude self-sustained oscillations in combustion organization systems characterized as thermoacoustic instability is one of the most complicated research fields. Even with the development of advanced measurement methods used in experiments and significant enhancement of computational resources necessary to describe the physical features of the flow in numerical investigations, it is not always possible to explain the dynamic characteristics and the associated complex flows [6, 7].

[a]Khristianovich Institute of Theoretical and Applied
 Mechanics, Siberian Branch, Russian Academy of Sciences,
 Novosibirsk, 630090 Russia; *nfed@itam.nsc.ru.

Interaction between the unsteady vortex motion and flame development can cause intense oscillations of temperature and pressure, which make the flow and combustion processes in a supersonic flow unstable. Instability increases as the heat release becomes more nonuniform [5]. Unstable combustion and possible resonance processes are accompanied by intense pressure oscillations in the channel and drastic changes in heat release in the combustion region [8].

Oscillations in the course of combustion in a supersonic flow were experimentally studied for configurations with a flameholder shaped as pylons, cavities, and backward-facing steps [8–10]. The measurements were limited by the Mach number of 2 and temperatures up to 1000 K. It was found that the basic reason for flow instability is associated not only with flame stabilization (flow separation), but also with internal instability of the flow field. Flame oscillations were measured on the basis of flow images taken with a high speed and pressure measurements in the combustor [10]. Various mechanisms responsible for instability dynamics were systematically studied [11].

Oscillations of combustion in a supersonic flow are affected by numerous factors: temperature at the combustor entrance, fuel type, and equivalence ratio [10, 12]. It was shown [12] that these factors can significantly affect flow interaction with shock waves in the channel, which generates low-velocity separation regions, and these factors correlate with the combustion intensity. Strong interaction of combustion and separated boundary layer further downstream increases the thermal region, leading to intensification of combustion of the mixture [13, 14].

Despite numerous investigations and successful solutions, it is still difficult to understand combustion instability in supersonic flows because of the complex structure of the flow, heat release nonuniformity, and influence of vibrational phenomena in supersonic combustion. Many studies were based on semi-empirical and phenomenological methods, but such approaches do not always provide acceptable solutions [15]. At the same time, it should be noted that these investigations were mainly performed at low Mach numbers at the channel entrance ranging from 1.5 to 2.5.

Much attention was paid to the methods of processing unsteady signals, which is extremely important in studying oscillations [16–19]. There are several analytical methods of determining the dynamic characteristics of the flow in the combustor, e.g., the fast Fourier transform (FFT) and dynamic mode decomposition (DMD) [17]. The short-time Fourier transform (STFT) is one of the methods derived from the FFT. The use of this approach is a reliable method of finding frequencies initiating combustion instability, which determines the beginning and transition to the dominating frequency on spectrograms [18]. The STFT results reveal the Fourier spectrum in the time series and are useful for tracing the transitions of the amplitude and frequency of pressure oscillations in time. Using the STFT and DMD methods, one can obtain the dynamics of acoustic oscillations, e.g., systems and shapes of 3D modes, and flame response to oscillations of various input parameters. These data are needed to monitor the emergence of instability and prevent engine failure or severe incidents.

Jin et al. [19] measured the flow fluctuations in the case of supersonic combustion and performed their frequency analysis. Temperature sensors measured the signals on the combustor walls. To analyze the temperature fluctuations, they used the continuous windowed Fourier transform, continuous windowed wavelet analysis, and windowed Hilbert–Huang transform. The sensor signal, which took into account the behavior of the wall temperature, was modeled in a one-dimensional formulation. This model signal was supplemented with random functions of three types; one with uniform noise only and two nonlinear distributions of fluctuations with respect to time with one linear segment at one time interval and an exponentially decreasing segment at another time interval. Jin et al. [19] used the Hilbert–Huang transform together with the empirical mode decomposition (EMD) [20], where the signal was divided into two components: empirical modes (fluctuations) and residual function. The Hilbert–Huang transform was applied only to empirical modes of fluctuations. Empirical decomposition of the signal was based on the search for envelopes over local maximums and local minimums with subsequent calculation of the centerline and fluctuations of the initial signal around this line. The EMD method was also used in [21] to describe the capabilities of this method in experimental gas dynamics by an example of the analysis of velocity oscillations in the wake behind a cylinder at subcritical Reynolds numbers.

The goal of the present paper was to measure and analyze pressure oscillations in the case of heat supply to the flow in a model channel with sudden expansion for the flow velocity at the channel entrance corresponding to the Mach number M = 3.85 under the conditions of unsteady ignition of the hydrogen–air mixture and subsequent transition to intense steady combustion. The main issues were choosing the methods for smoothing and filtration of signals obtained in the experiment, identifying pressure oscillations, comparing the intensity and frequency of oscillations in different combustion regimes, and determining the mutual effects of os-
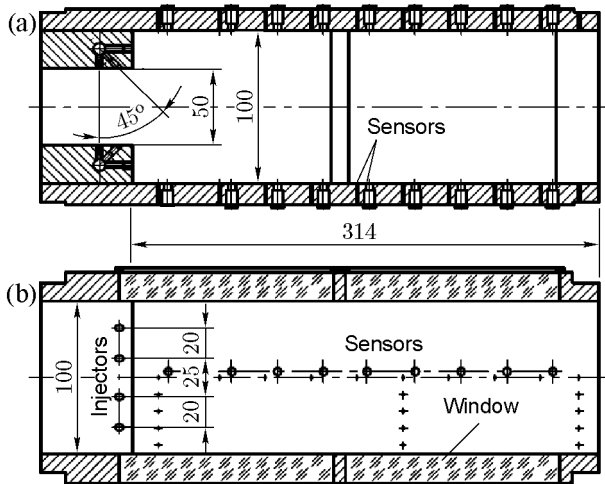
Fig. 1. Schematic image of the constant-section channel of the combustor in the longitudinal (a) and transverse (b) planes of symmetry.

Fig. 2. Behavior of the Mach number at the channel entrance during the run.

cillations on each other and their influence on the heat release efficiency.

EXPERIMENTAL SETUP, TEST CONDITIONS, AND MEASUREMENT METHODS

The experiments were performed in the IT-302M short-duration wind tunnel in the attached pipeline mode. The scheme with a throttling (second) chamber was used, which made it possible to vary the pressure at the model entrance and utilize the advantages of the hotshot wind tunnel as a source of a high-enthalpy test gas (air) to the greatest possible extent [22]. This wind tunnel is an effective tool for investigations of this kind because it ensures flow parameters close to flight conditions; moreover, the wind tunnel provides constant parameters of the flow during the run with the use of a pressure multiplier [23]. Such an approach ensures not only a required Mach number, but also required pressure and temperature at the combustor entrance in the entire range of test conditions

The experimental model was a rectangular channel 100 mm wide consisting of the nozzle part, isolator, and combustor. An injector section with a flameholder shaped as two symmetrically located steps 25 mm high was mounted at the combustor entrance (Fig. 1). Behind the injectors, there was a constant-section part of the channel (100 mm high and 314 mm long) and an expanding part of the channel 380 mm long with an expansion angle of 12° (not shown in the figure). Hydrogen was injected at an angle of 45° through eight
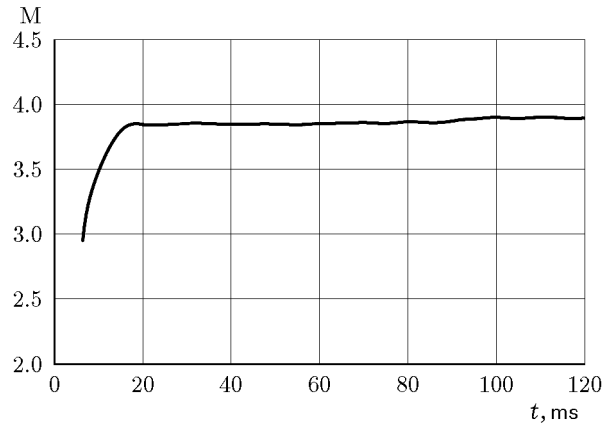
circular holes 2.6 mm in diameter located on the top and bottom walls of the channel ahead of the step at a distance of 8.5 mm from the leading edge.

The experimental studies were performed at supersonic velocities of air at the channel entrance without injection of hydrogen jets ("cold" flow) and with combustion induced by hydrogen injection into air ("hot" flow) in the regime without the pressure multiplier. During the run, we measured the total pressure and stagnation pressure in the settling and discharge chambers of the wind tunnel and also the static pressure and temperature at the channel entrance. The Mach number (M = 3.85) corresponding to the nominal value M = 4 was obtained on the basis of nozzle calibration and was determined in each test from the results of measuring the total pressure in the second chamber and the static pressure at the channel entrance ahead of the step. A typical example of the Mach number behavior in time is shown in Fig. 2. The change in the Mach number during the run was within ±0.8%. For determining the equivalence ratio, we calculated the mass flow rates of air and hydrogen based on the results of pressure and temperature measurements in the first chamber and in the fuel tank, respectively. Under conditions of gas exhaustion from a closed volume, this approach allows one to ignore the pressure loss in complex-shaped input channels and ensures acceptable accuracy of measurements, which was proved by calibrations.

An example of the static pressure (p_w) and temperature (T) measured under the present test conditions is shown in Fig. 3. It is seen that the most significant change in the time interval of 100 ms is the decrease in pressure (by more than a factor of 5), whereas the temperature decreases only by 55%. Though the Mach number remains almost constant during the experiment, the flow parameters decrease in time. The extent of this
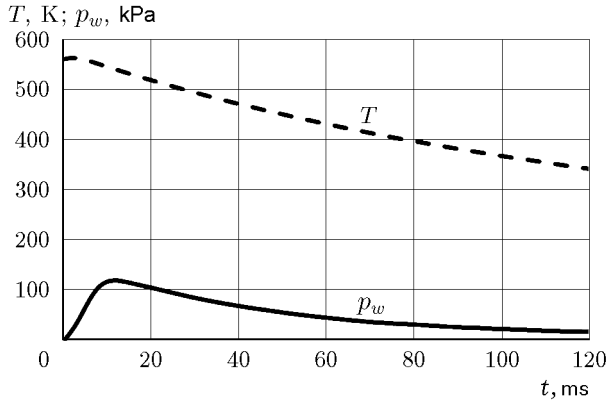
T, K; p_w, kPa

Fig. 3. Evolution of the static pressure and temperature during the run.

Table 1. Coordinates of pressure sensors located on the channel walls of the constant-section part of the channel

Sensor number	x, mm	Sensor number	x, mm
D1	17	D6	177
D2	57	D7	207
D3	87	D8	237
D4	117	D9	267
D5	147	D10	293

Table 2. Uncertainty of measurement of flow parameters

Parameter	Error, %
Total pressure	±0.83
Static pressure	±1.33
Total temperature	±1.57
Mach number	±1.27
Air flow rate	±2.58
Fuel flow rate	±1.79
Heat flux	±4.84
Time	±0.094

decrease depends on the Mach number and increases with a decrease in the Mach number.

The top and bottom walls of the channel accommodate static pressure and heat flux sensors. We used standard pressure sensors KPY-1U and KPY-4U with the nominal measurement values of 1 and 4 bar and with the declared measurement error of 0.2%. A three-fold calibration of all sensors was performed before each test series, which confirmed the declared accuracy of measurements. The certified ultimate frequency of 5 kHz was used as a dynamic characteristic of the sensors. The dynamic calibration of the pressure sensors showed that the response time at the pressure level reached in the present experiments was within 0.04–0.1 ms. The time step of the system of signal registration was 0.328 ms. This step was chosen in order to ensure operation of the needed number of sensors. As the sensor response time was significantly smaller than the time step, the parameters of the measurement system made it possible to study the pressure fluctuations in the frequency range up to 1.5 kHz, which was sufficient for determining the characteristic frequencies in the experiments.

The heat flux was measured by a sensor fabricated on the basis of the classical Gardon principle [24], which allows heat flux measurements up to 560 W/cm². The temperature was measured by Chromel–Alumel thermocouples (of the K type) with junction diameters of 0.05 and 0.1 mm, which allowed us to obtain an acceptable response time of the sensor for experiments in the short-duration wind tunnel. The working surface of the sensors was blackened before the measurements. All sensors were calibrated before the tests.

The coordinates of the sensors located in the constant-section part of the channel with respect to the step are listed in Table 1. Owing to a large number of measurement points, detailed distributions of the static

pressure and heat fluxes on the channel walls were obtained, including the base pressure and the pressure in transverse directions. The side wall of the combustor was equipped with optical glasses used for shadowgraphy and photographing the flame in the visible range.

The uncertainty of determining the flow parameters in the experiments was estimated by standard methods of the measurement accuracy analysis under the assumption that the confidence level was 95%. The uncertainty of measurement of various parameters is presented in Table 2.

EXPERIMENTAL RESULTS. SIGNAL PROCESSING METHOD

Figure 4 shows the behavior in the static pressure on the channel walls with time at points D1–D10 (see Table 1) in the "cold" (without combustion) and "hot" (with combustion) flows. These data illustrate the changes in pressure oscillations; a comparison of these data allowed us to estimate the influence of heat
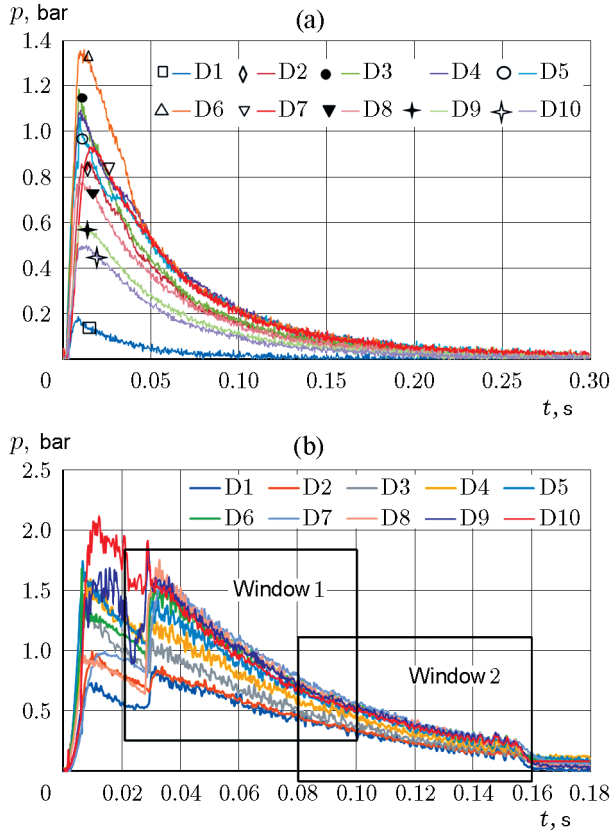
Fig. 4. Static pressure on the channel walls in experiments without combustion (a) and with combustion (b).

supply on the changes in the level of pressure fluctuations. Reduction of the static pressure during the run is related to specific features of the quasi-steady regime of high-enthalpy wind tunnels due to gas outflow from a closed volume [22].

In the test without combustion (Fig. 4a), the pressure monotonically decreases during the entire run. A detailed analysis of the flow structure under these conditions can be found in [25]. The data show that the pressure along the channel changes nonmonotonically and increases by a factor of 5–6. The maximum pressure is reached in the middle part of the channel (points D6 and D7; $x = 177$–207 mm), where the pressure increases due to the action of the tail shock reflected from the mixing layer, as was shown in [25]. At the same time, the estimates show that the intensity of pressure oscillations changes only slightly during the run.

Figure 4b illustrates the pressure behavior in the case with fuel combustion, resulting in an increase in pressure along the entire channel. The maximum pressure is reached approximately in the same region as in the run without combustion. It should be noted that

the pressure evolution in time has a nonmonotonic character because of the unsteady process of ignition and combustion stabilization. The most significant increase in pressure is observed in the base region behind the backward-facing step and in the region of the tail shock ($x = 17$–87 mm). Another specific feature of the flow with combustion is the fact that both the frequency and amplitude of oscillations change during the run, and these changes are different at all points along the channel.

The data of Fig. 4b were used to identify oscillations by two methods of signal filtration. As the present research is aimed at studying the influence of pressure oscillations on mixing and combustion in the channel, it is necessary to analyze the amplitude and frequency characteristics of the flow. To study the amplitude and frequency of pressure oscillations p' under the condition of essential unsteadiness of the mean values, the oscillating component was identified by means of subtracting the smoothed function from the original signal: $p' = p - \bar{p}$.

Two methods of obtaining the mean lines $\bar{p}$ were used to identify pressure oscillations. The first method is based on wavelet filtration of the original signal to decompose the latter into discrete Daubeshi wavelets DAUB8 [26, 27]. After that, filtration with rejection of small scales was performed, so that six large scales were retained, while four smallest scales were set to zero.

In the second method, the mean line was obtained by using smoothing splines [28]. The signal was approximated by a cubic spline with a controlled corridor around this line with a specified width (variance σ_i^2). Such a spline is constructed by means of minimizing the functional, which includes the norm of the second derivative of the spline (this part is responsible for the smoothness of the curve passing between the experimental points) and the norm of deviation of the experimental points from the mean line. In the present experiments, the corridor width was chosen to be $\sigma_i^2 = 4\%$ of the local amplitude of the signal in time.

Figure 5 shows the experimental values of pressure oscillations $p'(t)$ at various points on the channel walls in the "hot" flow, which were identified by using a smoothing spline (Fig. 5a) and wavelet filtration (Fig. 5b). The curve numbers correspond to the sensor numbers (see Table 1). Then the signals were processed by the fast Fourier transform [27]. As a result, the spectral densities of the signal power as functions of the oscillation frequency f were obtained.

A comparison of the results of oscillation identification by two methods by an example of several samples of experimental signals allowed us to conclude that the preferable method for determining the mean line in the
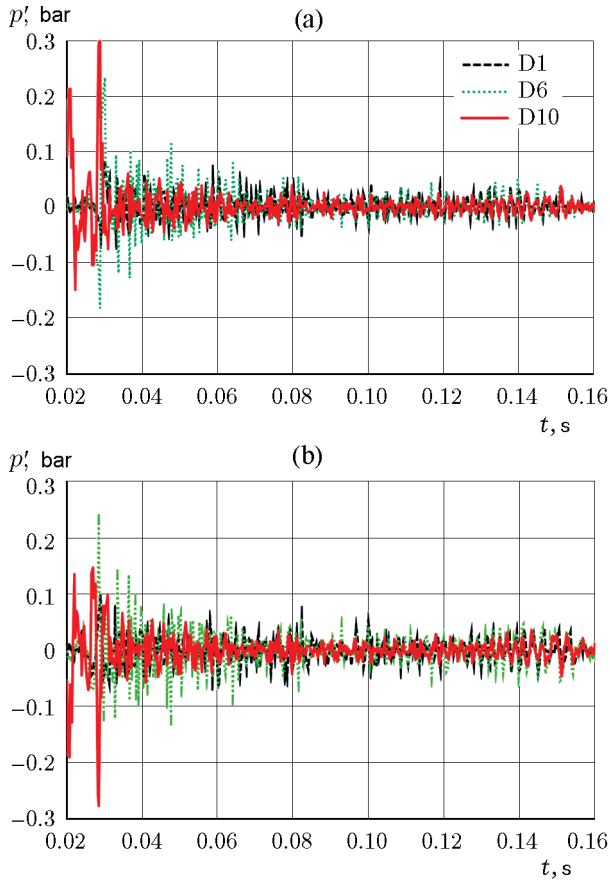
Fig. 5. Oscillations of the static pressure on the channel walls in experiments with combustion obtained by using a smoothing spline (a) and wavelet filtration (b).
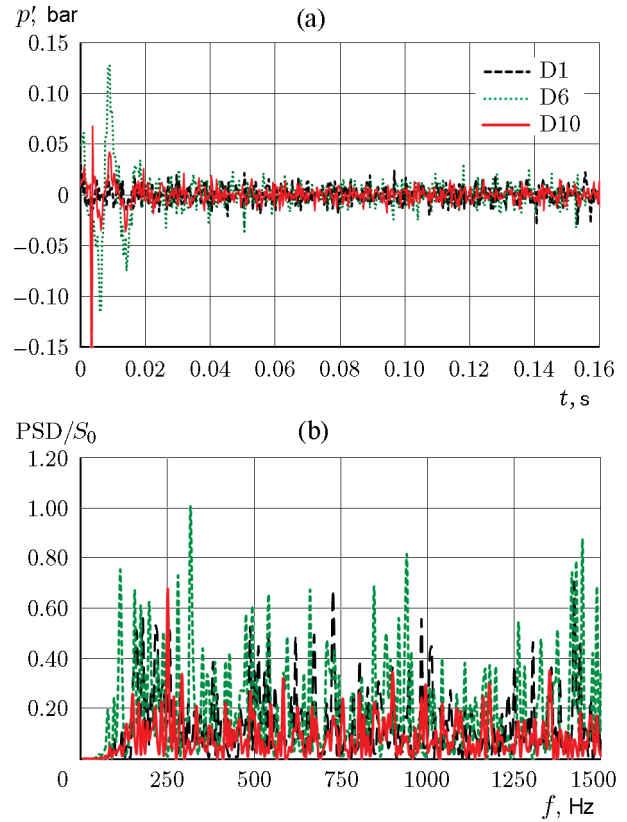

Fig. 6. Time evolution of static pressure oscillations (a) and normalized power spectral density of these oscillations (b) in the flow without combustion at three characteristic cross sections of the constant-section part of the channel.

present experiment is wavelet filtration. This method is used below in analyzing the oscillating characteristics of the flow.

Within the framework of the proposed approach, we analyzed the pressure oscillations in the run without combustion; the results are presented in Fig. 6. It is seen that the intensity of oscillations remains almost unchanged during the run. The increase in the amplitude of oscillations in the time interval from zero to 16 ms is caused by filling of the second chamber and associated wave processes, which rapidly decay. At the point D6 located in the middle part of the channel, one can observe an increase in the amplitude of oscillations owing to reattachment of the mixing layer behind the step.

To quantify the power spectral density (PSD) of the identified oscillations as a function of frequency, we used the fast Fourier transform (Fig. 6b). First of all, it should be noted that the maximum spectral density is reached in the middle part of the constant-section channel (D6 and D7; $x = 177$–207 mm),

where combustion initiation occurs, as was noted in [14]. The analysis of pressure oscillations in the "cold" flow revealed an elevated spectral power in three frequency ranges: 250–350, 900–1100, and 1400–1500 Hz. The PSD value was normalized to the maximum value $S_0 = 3 \cdot 10^{-3}$ kPa^2/Hz. As the study of time dependences obtained in short-duration wind tunnels is usually performed with dimensionless values normalized to the value of the corresponding parameter at the channel entrance, this PSD value is used below as a reference value for normalization of the spectral power of oscillations in the "hot" flow.

A comparison of the data in Figs. 4a and 4b testifies to significant differences in both the intensity and frequency of pressure oscillations in the case with combustion. Based on the analysis of Fig. 4b, it is possible to identify three characteristic periods of combustion:
• Initiation of combustion. Local combustion is observed at $t = 15$–27 ms with a moderate level of the pressure increase;
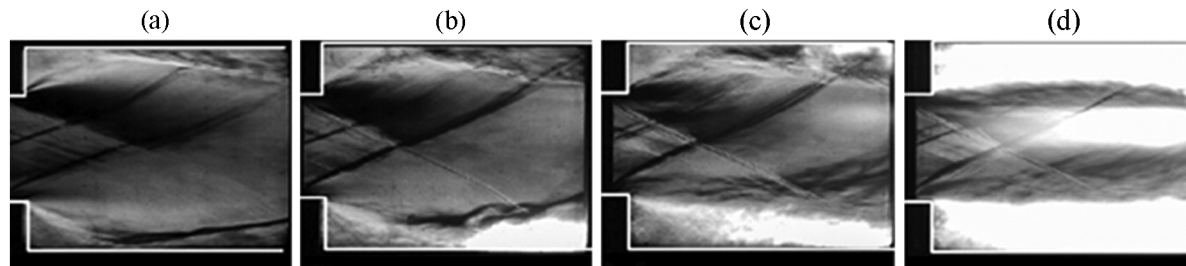
Fig. 7. Shadowgraphs of flame propagation along the channel at various time instants at the initial stage of ignition: the flow direction is from left to right; the light lines are the wall contours.

● Intensification of combustion, which begins from a drastic increase in pressure at $t \approx 27$ ms, and then the pressure gradually increases along the entire channel. This process is accompanied by upstream propagation of the flame front from the ignition region to the step;

● Period of steady combustion, which begins approximately at 120 ms and ends by combustion termination caused by the end of wind tunnel operation.

The photographs in Fig. 7 illustrate the motion of the flame front at the initial stage of local combustion from the instant of hydrogen injection into the flow up to the beginning of pressure increasing at 27 ms [14]. It is seen that the thickness of the layer with combustion increases as the flame propagates with time, and the heat release in the near-wall region gradually increases.

For the analysis of specific features of the development of flow oscillations during the transition to a steady regime, Fig. 8 shows the pressure oscillations in two time windows: $0.02 < t < 0.1$ s (see window 1 in Figs. 4b) and $0.08 < t < 0.16$ s (window 2). To facilitate understanding of data, we chose three characteristic cross sections along the channel, which representatively illustrate specific features of the processes in these regions. The windows are chosen to analyze the characteristics of the combustion process at different stages. To use the FFT algorithm for processing, both windows had an identical number of points (256).

One can see significant qualitative differences of oscillations in terms of their amplitude and frequency. First of all, we should note a strong increase in the amplitude at the instant of ignition at the end of the constant-section part of the channel (curve D10 in Fig. 8a) and low intensity of flow oscillations behind the step up to $t = 0.03$ s (curve D1 in Fig. 8a), which is a consequence of rapid expansion of the flow in the expansion fan. At the end of the period, one can see an extended region $t = 0.12$–0.15 s of vibrational (oscil-
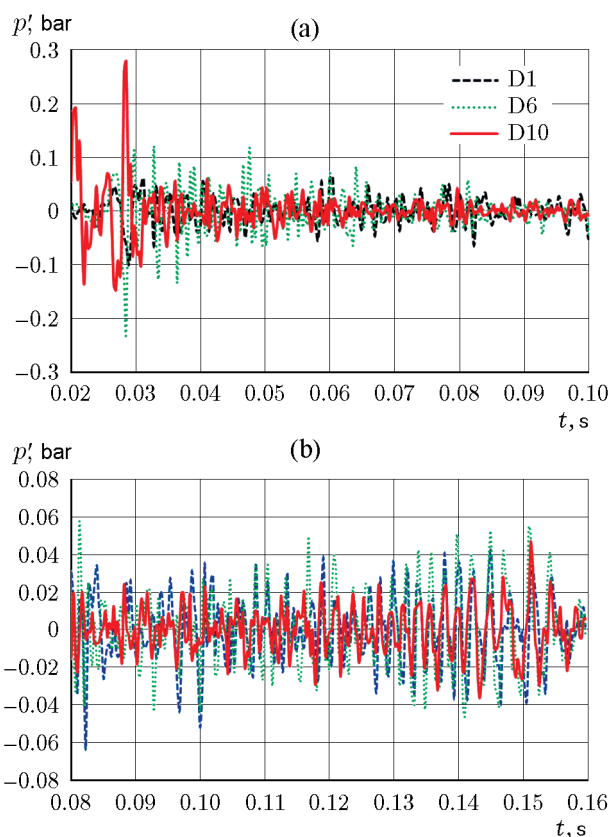

Fig. 8. Pressure oscillations identified with the use of wavelet filtration at various points on the channel walls in the "hot" flow for window 1 (a) and window 2 (b).

lating) combustion [15] characterized by simultaneous pressure oscillations along the channel with an increasing amplitude (Fig. 8b).

The normalized power spectral density of pressure oscillations in the "hot" flow obtained by using the FFT algorithm for windows 1 and 2 is shown in Fig. 9. In the
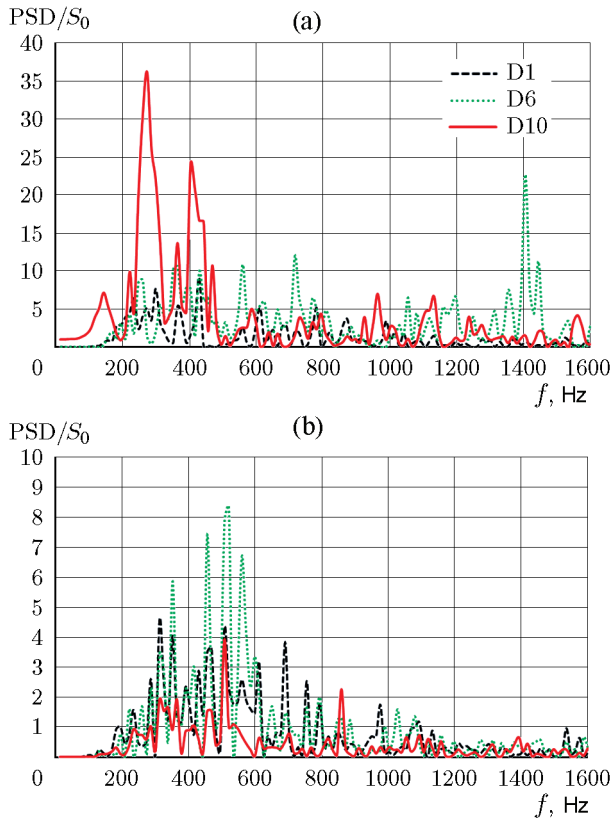
Fig. 9. Normalized power spectral density of pressure oscillations in the "hot" flow versus frequency for window 1 (a) and window 2 (b).

time interval corresponding to window 1 (Fig. 9a), one can see high-power oscillations in the frequency range from 250 to 400 Hz in the ignition region, which is located at the end of the constant-section part of the channel (between curves D6 and D10). A high frequency of 1440 Hz was obtained only in the middle of the channel (curve D6) with a comparatively low intensity of these oscillations. The pattern becomes different at the final stage of the process, which is characterized by enhanced heat release (Fig. 9b), where the maximum intensity of the spectrum of oscillations decreases by several times and the "peak" in the high-frequency region vanishes. Spectra of oscillations with frequencies in the range from 300 to 800 Hz and power greater than the reference value S_0 in the "cold" flow by a factor of 4–10 are observed over the entire channel. The maximum intensity of oscillations is reached at the center of the constant-section part of the channel (point D6) in the region of intense heat release, as was noted in [14].

Thus, owing to the upstream motion of the flame, which was studied in [29, 30] and enhancement of heat release resulting from intensification of chemical reac-

tions, the oscillations in the flow significantly increase. The analysis of pressure oscillations by the FFT algorithm shows (see Fig. 9) that the power spectral density of pressure oscillations increases approximately by a factor of 40 at the first stage and by a factor of 10 at the second stage of the development of the "hot" flow as compared to the nonreacting flow. As is seen from Fig. 9b, the maximum of the spectral density of oscillations is shifted at the end of the run upstream to the middle of the channel, $x = 147$–177 mm (between curves D5 and D6) and decreases by a factor of 4–5 as compared to the initial period. Simultaneously, the intensity of oscillations with frequencies higher than 600 Hz decreases, which is typical for flows with a high level of heat supply [15].

CONCLUSIONS

A series of experiments was performed to study the flow with a supersonic (M = 3.85) velocity at the channel entrance without and with heat supply. Power spectral densities of pressure oscillations were obtained on the basis of processing experimental results on the static pressure on the channel walls as a function of time. The analysis of these data showed that the spectral power of pressure oscillations in the case of combustion in the flow increases in the range from 250 to 400 Hz. The greatest increase in power as compared to the flow conditions without combustion was found to occur in the initial period of the process, during mixture ignition and flame stabilization on the backward-facing step. In the final period of combustion, which is limited by the run duration or pre-choking of the channel, the maximum spectral power of oscillations decreases, and the frequency range extends to the interval 400–600 Hz.

Subsequent investigations will be focused on studying the influence of the flow parameters on the oscillation characteristics and instability of the flow in self-oscillatory regimes and regimes with channel choking (transition to subsonic combustion) and on improvement of instrumental techniques and algorithms of signal processing in high-velocity unsteady flows.

REFERENCES

1. F. A. Williams, *Combustion Theory. The Fundamental Theory of Chemically Reacting Flow Systems* (CRC Press, 1994).

2. R. I. Sujith and V. R. Unni, "Dynamical Systems and Complex Systems Theory to Study Unsteady Combustion," Proc. Combust. Inst. **38** (3), 3445–3462 (2021); DOI: 10.1016/j.proci.2020.07.081.

3. F. S. Billig, "Research on Supersonic Combustion," J. Propul. Power **9** (4), 499–514 (1993); DOI: 10.2514/3.23652.

4. F. Ladeinde and W. Li, "Differential Turbulent Supersonic Combustion of Hydrogen, Methane, and Ethylene, without Assisted Ignition," AIAA J. **56** (12), 4870–4883 (2018); DOI: 10.2514/1.J057124.

5. J. Zhang, J. Chang, C. Kong, et al., "Flame Oscillation Characteristics in a Kerosene Fueled Dual Mode Combustor Equipped with Thin Strut Flameholder," Acta Astronaut. **161**, 222–233 (2019); DOI: 10.1016/j.actaastro.2019.05.037.

6. D. Baccarella, Q. Liu, B. McGann, et al., "Isolator-Combustor Interactions in a Circular Model Scramjet with Thermal and Non-Thermal Choking-Induced Unstart," J. Fluid Mech. **917** (A38), 1–36 (2021); DOI: 10.1017/jfm.2021.238.

7. Y. Cheng, T. Jin, K. Luo, et al., "Large Eddy Simulations of Spray Combustion Instability in an Aero-Engine Combustor at Elevated Temperature and Pressure," Aerosp. Sci. Technol. **108**, 106329 (2021); DOI: 10.1016/j.ast.2020.106329.

8. K.-C. Lin, K. Jackson, R. Behdadnia, et al., "Acoustic Characterization of an Ethylene-Fueled Scramjet Combustor with a Cavity Flameholder," J. Propul. Power **26** (6), 1161–1169 (2010); DOI: 10.2514/1.43338.

9. H. Ouyang, W. Liu, and M. Sun, "The Large-Amplitude Combustion Oscillation in a Single-Side Expansion Scramjet Combustor," Acta Astronaut. **117**, 90–98 (2015); DOI: 10.1016/j.actaastro.2015.07.016.

10. H. M. Altay, L. E. Hudgins, and A. F. Ghoniem, "The Impact of Equivalence Ratio Oscillations on Combustion Dynamics in a Backward-Facing Step Combustor," Combust. Flame **156**, 2106–2116 (2009); DOI: 10.1016/j.combustflame.2009.07.024.

11. S. T. Ducruix, T. Schuller, D. Durox, and S. Candel, "Combustion Dynamics and Instabilities: Elementary Coupling and Driving Mechanisms," J. Propul. Power **19** (5), 722–734 (2003); DOI: 10.2514/2.6182.

12. J. Zhang and A. Ratner, "Experimental Study of the Effects of Hydrogen Addition on the Thermoacoustic Instability in a Variable-Length Combustor," Int. J. Hydrogen Energy **46** (29), 16086–16101 (2021); DOI: 10.1016/j.ijhydene.2021.02.063.

13. G.-Y. Zhao, M.-B. Sun, Y.-N. Wang, et al., "Investigations of Injection Parameters on Combustion Oscillation in Supersonic Crossflow," Acta Astronaut. **152**, 426–436 (2018); DOI: 10.1016/j.actaastro.2018.08.041.

14. M. A. Goldfeld, "Processes of Self-Ignition and Flame Stabilization with Transverse Hydrogen Fuel Injection into a Supersonic Combustion Chamber," Teplofiz. Aeromekh. **27** (4), 601–613 (2020) [Thermophys. Aeromech. **27** (4), 573–584 (2020)].

15. M. Sun, H. Wang, Z. Cai, and J. Zhu, *Unsteady Supersonic Combustion* (Springer, 2020); DOI: 10.1007/978-981-15-3595-6.

16. H. T. Luong, Y. Wang, H. S. Han, and C. H. Sohn, "Combined Applications of Analytic Methods for Detection of Combustion Instability Triggering," Aerospace Sci. Technol. **118**, 106994 (2021); DOI: 10.1016/j.ast.2021.106994.

17. S. M. Rao and S. Karthick, "Studies on the Effect of Imaging Parameters on Dynamic Mode Decomposition of Time-Resolved Schlieren Flow Images," Aerospace Sci. Technol. **88**, 136–146 (2019); DOI: 10.1016/j.ast.2019.03.004.

18. V. Dekys, P. Kalman, P. Hanak, et al., "Determination of Vibration Sources by Using STFT," Procedia Eng. **177**, 496–501 (2017); DOI: 10.1016/j.proeng.2017.02.251.

19. X. Jin, Y. Tian, K. Zhao, et al., "Experimental Study on Supersonic Combustion Fluctuation Using Thin-Film Thermocouple and Time–Frequency Analysis," Acta Astronaut. **179**, 33–41 (2021); DOI: 10.1016/j.actaastro.2020.09.041.

20. N. E. Huang, Z. Shen, S. R. Long, et al., "The Empirical Mode Decomposition and the Hilbert Spectrum for Nonlinear and Non-Stationary Time Series Analysis," Proc. R. Soc. London, A **454** (1971), 903–995 (1998); DOI: 10.1098/rspa.1998.0193.

21. D. S. Mironov, V. A. Lebiga, D. D. Miau, et al., "Application of the Hilbert–Huang Transform for the Analysis of Fluctuations behind a Straight Circular Cylinder," Sib. Fiz. Zh. **12** (3), 49–59 (2017).

22. M. A. Goldfeld, A. A. Maslov, A. V. Starov, et al., "IT-302M Hotshot Wind Tunnel as a Tool for the Development of Hypersonic Technologies," AIP Conf. Proc. **1770**, 030020 (2016); DOI: 10.1063/1.4963962.

23. A. A. Maslov, V. V. Shumskii, and M. I. Yaroslavtsev, "High-Enthalpy Hot-Shot Wind Tunnel with Combined Heating and Stabilization of Parameters," Teplofiz. Aeromekh. **20** (5), 535–546 (2013) [Thermophys. Aeromech. **20** (5), 527–538 (2013)].

24. T. E. Diller, "Advances in Heat Flux Measurements," Adv. Heat Transfer **23**, 279–368 (1993); DOI: 10.1016/S0065-2717(08)70008-X.

25. M. A. Goldfeld, Yu. V. Zakharova, A. V. Fedorov, and N. N. Fedorova, "Effect of the Wave Structure of the Flow in a Supersonic Combustor on Ignition and Flame Stabilization," Fiz. Goreniya Vzryva **54** (6), 3–16 (2018) [Combust., Expl., Shock Waves **54** (6), 629–641 (2018); DOI: 10.1134/S0010508218060011].

26. N. M. Astaf'eva, "Wavelet Analysis: Basic Theory and Some Applications," Usp. Fiz. Nauk **166**, 1145–1170 (1996) [Phys.-Usp. **39** (11), 1085–1108 (1996); DOI: 10.1070/PU1996v039n11ABEH000111].

27. W. H. Press, S. A. Teukolsky, W. T. Vetterling, and B. P. Flannery, *Numerical Recipes in FORTRAN* (Cambridge Univ. Press, Cambridge, 1992).

28. Yu. E. Voskoboinikov, "Construction of Smoothing Cubic Splines in Machine Processing of Experimental Results," Avtometriya, No. 4, 110–117 (1979).

29. J. Zhang, J. Chang, Z. Wang, et al., "Flame Propagation and Flashback Characteristics in a Kerosene Fueled Supersonic Combustor Equipped with Strut/Wall Combined Fuel Injectors," Aerosp. Sci. Technol. **93**, 105303 (2019); DOI: 10.1016/j.ast.2019.105303.

30. N. N. Fedorova, O.S. Vankova, and M. A. Goldfeld, "Unsteady Regimes of Hydrogen Ignition and Flame Stabilization in a Channel," Fiz. Goreniya Vzryva **58** (2), 3–11 (2022) [Combust., Expl., Shock Waves **58** (2), 127–134 (2022); DOI: 10.1134/S0010508222020010].